



Modelling contrasting responses of wetland productivity to changes in water table depth

R. F. Grant¹, A. R. Desai², and B. N. Sulman²

¹Department of Renewable Resources, University of Alberta, Edmonton, AB, Canada

²University of Wisconsin-Madison Department of Atmospheric and Oceanic Sciences, 1225 W. Dayton St, Madison, WI 53706, USA

Correspondence to: R. F. Grant (robert.grant@ales.ualberta.ca)

Received: 15 April 2012 – Published in Biogeosciences Discuss.: 14 May 2012

Revised: 17 September 2012 – Accepted: 21 September 2012 – Published: 1 November 2012

Abstract. Responses of wetland productivity to changes in water table depth (WTD) are controlled by complex interactions among several soil and plant processes, and hence are site-specific rather than general in nature. Hydrological controls on wetland productivity were studied by representing these interactions in connected hummock and hollow sites in the ecosystem model *ecosys*, and by testing CO₂ and energy fluxes from the model with those measured by eddy covariance (EC) during years with contrasting WTD in a shrub fen at Lost Creek, WI. Modelled interactions among coupled processes for O₂ transfer, O₂ uptake, C oxidation, N mineralization, N uptake and C fixation by diverse microbial, root and mycorrhizal populations enabled the model to simulate complex responses of CO₂ exchange to changes in WTD that depended on the WTD at which change was occurring. At the site scale, greater WTD caused the model to simulate greater CO₂ influxes and effluxes over hummocks vs. hollows, as has been found at field sites. At the landscape scale, greater WTD caused the model to simulate greater diurnal CO₂ influxes and effluxes under cooler weather when water tables were shallow, but also smaller diurnal CO₂ influxes and effluxes under warmer weather when water tables were deeper, as was also apparent in the EC flux measurements. At an annual time scale, these diurnal responses to WTD in the model caused lower net primary productivity (NPP) and heterotrophic respiration (R_h), but higher net ecosystem productivity ($NEP = NPP - R_h$), to be simulated in a cooler year with a shallower water table than in a warmer year with a deeper one. This difference in NEP was consistent with those estimated from gap-filled EC fluxes in years with different water tables at Lost Creek and at similar boreal fens

elsewhere. In sensitivity tests of the model, annual NEP declined with increasing WTD in a year with a shallow water table, but rose in a year with a deeper one. The model thus provided an integrated set of hypotheses for explaining site-specific and sometimes contrasting responses of wetland productivity to changes in WTD as found in different field experiments.

1 Introduction

The productivity of wetland ecosystems is strongly affected by changes in water table depth (WTD). However, these effects are complex and site-specific because they arise from numerous interactions among physical and biological processes that control carbon and nutrient transformations in soils. Lowering shallow water tables has been found to increase soil respiration (Flanagan and Syed, 2011; Silvola et al., 1996) through the effects of increased access to O₂ on microbial activity in drained soil (Moore and Dalva, 1993). However, lowering deeper water tables has been found not to affect, or even to reduce, soil respiration (Lafleur et al., 2005; Muhr et al., 2011; Scanlon and Moore, 2000) because effects on microbial activity from increased uptake of O₂ in deeper drained soil may be offset by those from reduced access to substrates in dry surface soil (Dimitrov et al., 2010a).

The relationship between WTD and soil respiration therefore depends on the hydrological and biological properties of wetland soils. Those with large water holding capacity and low macroporosity drain more slowly, and so maintain soil wetness through capillary rise, enabling soil respiration to

increase as water tables deepen. Soils with low water holding capacity and large macroporosity drain more rapidly, and so are less able to maintain surface wetness through capillary rise, causing soil respiration not to increase, or even to decrease, as water tables deepen. The extent to which respiration increases in soils drained by deepening water tables also depends upon the lability vs. recalcitrance (Muhr et al., 2011; Nadelhoffer et al., 1991) and on the temperature (Blodau et al., 2007) of the deeper drained soil organic carbon (SOC).

More rapid soil respiration with greater WTD can hasten nutrient mineralization and uptake, and thereby increase primary productivity. Wood and foliar growth are more rapid on soils with lower water tables because nutrient mineralization and consequently nutrient uptake are more rapid, as evidenced by higher foliar nutrient concentrations and CO₂ assimilation rates measured in spruce on drained vs. undrained peatlands (Macdonald and Lieffers, 1990) or in a treed fen over declining water tables (Flanagan and Syed, 2011). Lowering of water tables has caused annual basal area increments of black spruce to more than double (Lieffers and Macdonald, 1990) and annual tree ring growth to increase by several times (Dang and Lieffers, 1989) at different boreal sites. More rapid nutrient uptake and growth with lower water tables have been attributed to higher soil temperatures (Lieffers and Rothwell, 1987) and lower soil water contents (Lieffers, 1988). More rapid nutrient uptake and growth can also be attributed to more rapid root O₂ uptake and hence activity, particularly in roots with low internal porosity which rely more on soil transport for O₂ uptake. However, in soils with rapid drainage and low water holding capacity, lower water tables can reduce productivity by causing surface drying and hence water stress in shallow-rooted vegetation such as moss (Dimitrov et al., 2011).

Responses of respiration and productivity to changes in water table thus depend upon soil and plant properties as well as on WTD, and consequently differ among wetlands (Adkinson et al., 2011; Sulman et al., 2010). Mathematical models may provide a means to understand and eventually to predict these responses, but only if they represent the basic processes by which these responses are determined. Water table effects on soil respiration are usually represented in models by lower rate constants for anoxic decomposition (Clymo, 1992; St-Hilaire et al., 2010), or by scalar functions that reduce rate constants for decomposition at high soil water contents or potentials (e.g. Bond-Lamberty et al., 2007; Zhang et al., 2002). Water table effects on productivity are sometimes represented by time-dependent scalar functions that reduce productivity in wet soils through a driver variable such as stomatal conductance (e.g. Bond-Lamberty et al., 2007; Sonnentag et al., 2008). However, these scalar functions do not simulate the physical and biological processes by which suppression of decomposition and productivity occur in wetland soils, but rather the effects of these processes.

Even so, these functions are not widely implemented in mathematical models used to study ecosystem behavior. In a recent review of seven widely used ecosystem models, Sulman et al. (2012) found only one which included processes to limit productivity in wet soils. Furthermore, most ecosystem models do not simulate the hydrological processes that control WTD and hence the soil wetness that drives these functions, but rather require WTD as an input (e.g. St-Hilaire et al., 2010; Frohling et al., 2002). This requirement limits the predictive capabilities of these models.

The key processes needed in models used for studies of wetland productivity are the transport, uptake and reduction of O₂ in soil as affected by soil water content. Higher water tables are thought to decrease respiration by reducing O₂ uptake used to drive oxidation–reduction reactions by soil microbes and roots. Energy yield from oxidation when coupled to reduction of O₂ exceeds that from oxidation when coupled to reduction of other electron acceptors (Brock and Madigan, 1991). Reduced O₂ uptake therefore slows processes driven by this energy, including microbial and root growth, decomposition and nutrient mineralization, and hence nutrient uptake and plant productivity. On the other hand, lower water tables are thought to decrease respiration by reducing microbial access to substrate in desiccated near-surface soil (Dimitrov et al., 2010a), thereby slowing oxidation–reduction reactions and hence microbial growth and activity. Models used to study water table effects on wetland respiration and productivity therefore should explicitly simulate (1) the transformations and energy yields of oxidation–reduction reactions by microbes and roots, (2) controls on the rates of these reactions exerted by the transfers of water and of the reactants and products of these reactions, particularly O₂, through soil and roots, and (3) the effects of these reactions on soil nutrient transformations and root nutrient uptake. These reactions, as well as their controls and effects, need to be simulated in dynamic aerobic and anaerobic zones determined by water table position calculated from vertical and lateral water transfers.

These processes are implemented to varying degrees in transient variably saturated flow models (e.g. Langergraber and Šimůnek, 2005) used to study respiration in constructed wetlands. The full implementation of these processes would avoid the arbitrary scalar functions described above which are used to represent these effects in some current ecosystem models. Such implementation is attempted in the general-purpose model *ecosys*, in which a comprehensive set of oxidation–reduction reactions in soil (obligate aerobic, facultative anaerobic and obligate anaerobic heterotrophic decomposition, heterotrophic and autotrophic methanogenesis, autotrophic methanotrophy, autotrophic nitrification and heterotrophic diazotrophy) and roots are calculated from reaction kinetics driven by oxidation–reduction energy yields (Grant, 1998, 1999; Grant and Pattey, 2003; Grant et al., 2006, 2009b, 2009a, 2010a, b). All reactants and products of these reactions undergo convective–dispersive

transfer through, and volatilization–dissolution exchange between, gaseous and aqueous phases of soil and roots in three-dimensional soil landscapes, thereby controlling aqueous concentrations and hence oxidation–reduction rates (Dimitrov et al., 2010a, 2011; Grant, 2004; Grant and Roulet, 2002). These rates drive those of soil nutrient transformations and hence root nutrient uptake, thereby controlling primary productivity (Grant et al., 2009a, 2010a, b). All algorithms used to simulate these transformations and transfers are parameterized from basic research conducted independently of the model, allowing *ecosys* to avoid arbitrary parameterizations of anaerobic effects on respiration and productivity used in earlier models. Furthermore, the model includes a full set of vertical and lateral water flows used to calculate WTD (Dimitrov et al., 2010b; Grant, 2004), enabling the simulation of all key processes by which WTD affects wetland respiration and productivity.

The absence of these processes in most ecosystem models prevents them from simulating changes in respiration and productivity observed with changes in WTD, limiting their ability to simulate wetland behavior (Sulman et al., 2012). The objective of this study is to determine whether implementing these processes in a more detailed ecosystem model such as *ecosys* would enable simulation of the complex changes in wetland respiration and productivity observed with changes in WTD. For example, with greater WTD the model should be able to simulate increases in respiration from more rapid O₂ uptake and reduction under some conditions, but decreases in respiration from soil drying under others. With greater WTD the model should also be able to simulate increases in productivity from more rapid nutrient mineralization and uptake under some conditions, but reduced productivity from water stress under others. To accomplish this, CO₂ fluxes modelled over a shrub fen at Lost Creek, WI were compared with those measured by eddy covariance (EC) at hourly, seasonal and annual time scales during several years with differing temperature, precipitation and WTD.

2 Methods

2.1 Model development

2.1.1 General

The key algorithms governing the modelling of ecological controls on CO₂ exchange in *ecosys* are described in the Supplement to this article, in which equations and variables referenced below are described and listed in Appendices A through F. Algorithms which govern the transport, uptake and reduction of O₂ in soil are particularly relevant to controls on CO₂ exchange in wetlands, and so are described here in further detail. All model parameters in *ecosys* are derived from independent experiments and so remain unchanged in

this study from those used in earlier studies (e.g. Dimitrov et al., 2010a, b, 2011; Grant, 2004; Grant et al., 2009a, b, 2010a, b, 2011, 2012) as given in the Supplement.

2.1.2 Heterotrophic respiration

Organic transformations in *ecosys* occur in five organic matter–microbe complexes (coarse woody litter, fine non-woody litter, animal manure, particulate organic carbon (POC), and humus), each of which consists of five organic states (three decomposition substrates: solid organic C, sorbed organic C and microbial residue C, as well as the decomposition product: dissolved organic C (DOC), and the decomposition agent: microbial biomass) in a surface residue layer and in each soil layer. The decomposition rates of each of the three substrates and resulting production of DOC in each complex is a first-order function of the active biomasses M of diverse heterotrophic microbial functional types, including obligate aerobes (bacteria and fungi), facultative anaerobes (denitrifiers), obligate anaerobes (fermenters), heterotrophic (acetotrophic) and autotrophic (hydrogenotrophic) methanogens, and aerobic and anaerobic heterotrophic diazotrophs (non-symbiotic N₂ fixers) [A1, A2]. Decomposition rates are also Monod functions of substrate C concentrations in soil [A3], calculated from the fraction of substrate mass colonized by M [A4].

Growth of M by each microbial functional type [A25] is calculated from its uptake of DOC [A21], driven by energy yields from growth respiration (R_g) [A20] remaining after subtracting maintenance respiration (R_m) [A18] from heterotrophic respiration (R_h) [A11] driven by DOC oxidation [A13]. This oxidation may be limited by microbial O₂ reduction [A14] driven from microbial O₂ demand [A16] and constrained by aqueous O₂ concentrations ([O_{2s}]) [A17]. These concentrations are maintained by convective–dispersive transport of O₂ from the atmosphere to gaseous and aqueous phases in the soil surface layer [D15], by convective–dispersive transport of O₂ through gaseous and aqueous phases in adjacent soil layers [D16, D19], and by dissolution of O₂ from gaseous to aqueous phases within each soil layer [D14a].

Under dryland conditions, rapid O₂ diffusivity in the gaseous phase (D_g in [D17]) allows O₂ demand by aerobic functional types to be met almost entirely from [O_{2s}] [A17] as long as some air-filled porosity θ_g is present. However, with higher water tables, θ_g above the water table may decline to values at which D_g may reduce gaseous O₂ transport [D16], while θ_g below the water table is zero and so prevents gaseous O₂ transport. Under these conditions, [O_{2s}] relies more on O₂ transport through the slower aqueous phase [D19]. Consequent declines in [O_{2s}] slow O₂ uptake [A17] and hence R_h [A14], R_g [A20] and growth of M [A25]. Lower M in turn slows decomposition of organic C [A1, A2] and production of DOC, which further slows R_h [A13], R_g and growth of M . Although some microbial

functional types can sustain DOC oxidation by reducing alternative electron acceptors (e.g. methanogens reducing acetate or CO_2 to CH_4 in Grant, 1998, and denitrifiers reducing NO_x to N_2O or N_2 in Grant et al., 2006), lower energy yields from these reactions reduce DOC uptake from R_g , and hence M growth, organic C decomposition and subsequent DOC oxidation. Slower decomposition of organic C under low $[\text{O}_{2s}]$ also causes slower decomposition of organic N and P [A7] and production of DON and DOP, which causes slower uptake [A22] and growth [A29] of microbial N and P. This slower growth causes slower mineralization of NH_4^+ , NO_3^- and H_2PO_4^- [A26], and hence lower aqueous concentrations.

2.1.3 Autotrophic respiration

Growth of root and shoot phytomass in each plant population is calculated from its assimilation of the nonstructural C product of CO_2 fixation (σ_C) [C20]. Assimilation is driven by growth respiration (R_g) [C17] remaining after subtracting maintenance respiration (R_m) [C16] from autotrophic respiration (R_a) [C13] from oxidation of σ_C [C14]. This oxidation in roots may be limited by root O_2 reduction [C14b] which is driven by root O_2 demand to sustain C oxidation and nutrient uptake [C14e], and constrained by O_2 uptake controlled by concentrations of aqueous O_2 in the soil ($[\text{O}_{2s}]$) and roots ($[\text{O}_{2r}]$) [C14d]. Values of $[\text{O}_{2s}]$ are maintained by convective–dispersive transport of O_2 through soil gaseous and aqueous phases and by dissolution of O_2 from soil gaseous to aqueous phases through processes analogous to those described under *Heterotrophic Respiration* above. Values of $[\text{O}_{2r}]$ are maintained by convective–dispersive transport of O_2 through the root gaseous phase [D16d] and by dissolution of O_2 from root gaseous to aqueous phases [D14b]. This transport depends on species-specific values used for root air-filled porosity (θ_{pr}) [D17b].

Under dryland conditions, rapid O_2 diffusivity in the soil gaseous phase usually allows root O_2 demand to be almost entirely met from $[\text{O}_{2s}]$ [C14c, d] as long as some air-filled porosity θ_g is present. However, with higher water tables, reduced soil O_2 transport forces root O_2 uptake to rely more on $[\text{O}_{2r}]$ and hence on root O_2 transport. If this transport is inadequate, declines in $[\text{O}_{2r}]$ slow O_2 uptake [C14c, d] and hence R_a [C14b], R_g [C17] and root growth [C20b].

2.1.4 Primary productivity

When higher water tables reduce soil O_2 transport and root O_2 uptake, commensurate reductions in root C oxidation slow root growth and root N and P uptake [C23b, d, f]. Root uptake is further slowed by reductions in aqueous concentrations of NH_4^+ , NO_3^- and H_2PO_4^- [C23a, c, e] from slower mineralization of organic N and P as described in *Heterotrophic Respiration* above. Slower root uptake reduces concentrations of nonstructural N and C products of root up-

take (σ_N and σ_P) with respect to that of σ_C in leaves [C11], thereby slowing CO_2 fixation [C6] and hence productivity.

Thus, water table effects on R_h , R_a and productivity in *ecosys* are not explicitly parameterized from ecosystem-level observations, but instead are governed by O_2 transport and uptake through processes parameterized from basic research.

2.1.5 Water table depth

The position of the water table arises from influxes vs. effluxes of water in vertical and lateral directions within the landscape and through surface and subsurface boundaries in one-, two- or three-dimensions. Vertical surface boundary influxes from precipitation or irrigation are provided as inputs to the model. Vertical surface boundary effluxes from transpiration [B1] and evaporation [D6] are calculated from energy balances for canopy, snow, residue and soil surfaces [D11] coupled with subsurface water transfers through root [B5] and soil [D7] profiles. Lateral surface runoff within the landscape and across lower surface boundaries is modelled using Manning's equation [D1] with surface water velocity [D3] calculated from surface geometry [D5] and slope [D6], and with surface water depth [D2] calculated from surface water balance [D4] using kinematic wave theory. Vertical and lateral subsurface water flows within the landscape [D7] are calculated from Richard's equation using bulk soil water potentials ψ_s of adjacent cells if both source and destination cells are unsaturated [D9a], or from Green-Ampt equation using ψ_s beyond the wetting front of the unsaturated cell if either source or destination cell is saturated [D9b] (Grant et al., 2004). Vertical and lateral subsurface water flows can also occur within the landscape through macropores using Poiseuille-Hagen theory for laminar flow in tubes, depending on inputs for macropore volume fraction (Dimitrov et al., 2010b).

Lateral flows through subsurface boundaries are controlled by the depth of and distance to an external water table used to represent watershed effects on landscape hydrology (Fig. 1). The depth of this external water table is calculated as the average of a fixed value provided to the model, and the WTD in the boundary grid cells through which lateral flows occur. The external water table can therefore rise and fall with changes in landscape surface water exchange. Lateral subsurface flows from boundary grid cells are calculated from their ψ_s and lateral hydraulic conductivities, and from external hydraulic gradients determined by elevation differences and lateral distances between these grid cells and the external water table [D10]. The WTDs within the boundary grid cells are calculated from the uppermost position in the soil profiles at which discharge to, or recharge from, the external water table is occurring. The WTDs in the modelled landscape are not therefore prescribed, but are controlled by vertical surface boundary fluxes, and by lateral surface and subsurface boundary fluxes.

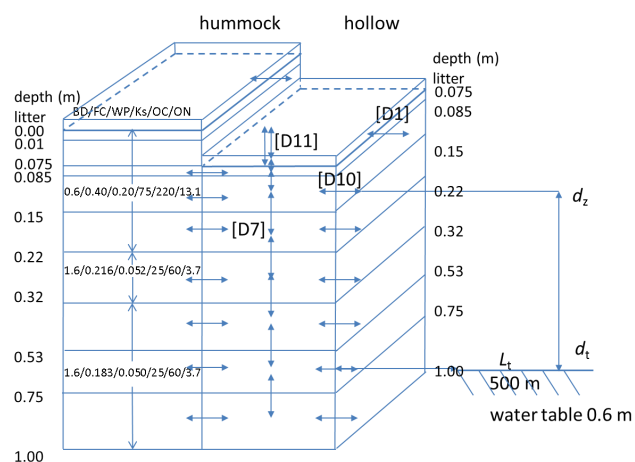


Fig. 1. Schematic representation of wetland landscape in *ecosys*. Depths are from the hummock surface to the bottom of each soil layer. Numbers in each soil layer are BD: Bulk density (Mg m^{-3}), FC: field capacity ($\text{m}^3 \text{m}^{-3}$), WP: wilting point ($\text{m}^3 \text{m}^{-3}$), Ks: saturated hydraulic conductivity (mm h^{-1}), OC: organic carbon (kg Mg^{-1}), ON: organic nitrogen (kg Mg^{-1}). Values for BD, OC and ON were measured at the field site. Values for FC, WP and Ks in the organic layers were derived from generalized relationships in Boelter 1969) and Päivänen (1973), and those in the mineral layers from pedotransfer functions in Saxton et al. (1986). L_t is distance to the external water table, d_z and d_t are depths of the internal (variable) and external (constant) water tables. Expressions in square brackets refer to equations in the Supplement by which indicated fluxes are calculated.

2.2 Model experiment

2.2.1 Site conditions

Model algorithms for the effects of hydrology on wetland respiration and productivity were tested with CO_2 fluxes measured by EC over a minerotrophic wetland dominated by alder (*Alnus incana* sp. *rugosa*) and willow (*Salix* sp.) shrubs with an understory of sedges (*Carex* sp.), near Lost Creek, WI ($46^\circ 4.90' \text{ N}$, $89^\circ 58.70' \text{ W}$) during six years (2001–2006) with contrasting weather and hydrology. The site and EC flux measurements are described in further detail by Sulman et al. (2009).

2.2.2 Model runs

Wetland microtopography was simulated by two interconnected soil profiles representing a hummock and a hollow, with equal areas and identical properties except for the absence of the upper 0.075 m in the hollow (Fig. 1). Based on site observations of WTD, the external water table was set to a depth of 0.6 m at a distance of 500 m from the modelled landscape (Fig. 1). Both the hummock and the hollow were seeded with the same populations of shrubs and sedges, properties of which were unchanged from those in earlier studies

(e.g. Dimitrov et al., 2011; Grant et al., 2003, 2011, 2012). Shrubs and sedges used common values for parameters in all autotrophic C transformations [C1–C23], except for 0.1 and 0.2 (Visser et al., 2000), respectively, for θ_{pr} in root O_2 transport [D17d]. The model was run for 105 yr under repeating 7-yr sequences of hourly-averaged weather data (solar radiation, air temperature, wind speed, humidity and precipitation) recorded at nearby Willow Creek in 2000, and at Lost Creek from 2001 to 2006. This period allowed CO_2 exchange in the model to achieve stable values through successive weather sequences. Model results for the final 6 yr of the run were compared with measurements at Lost Creek from 2001 to 2006.

2.2.3 Model testing

Hourly CO_2 fluxes modelled over the interconnected hummocks and hollows (Fig. 1) were averaged, based on similar areas of hummocks and hollows observed at the experimental site, and then regressed on hourly-averaged EC CO_2 fluxes, of which both 1/2-hourly values were measured rather than gap-filled, for each year of measurement. Model performance was evaluated from regression intercepts ($a \rightarrow 0$), slopes ($b \rightarrow 1$) and correlation coefficients ($R^2 \rightarrow 1$).

2.2.4 Model sensitivity to WTD

To examine sensitivity of modelled CO_2 exchange and productivity to changes in WTD, the final 6 yr of the model run described above were repeated with the depth of the external water table raised from 0.6 to 0.3 m, or lowered to 0.9 m, but with everything else unchanged.

3 Results

3.1 Modelled vs. measured CO_2 fluxes

Regressions of hourly modelled CO_2 fluxes averaged for the interconnected hummocks and hollows vs. hourly-averaged measured CO_2 fluxes gave intercepts within $0.1 \mu\text{mol m}^{-2} \text{ s}^{-1}$ of zero, and slopes within 0.1 of one, indicating minimal bias in modelled values for all years of the study except 2004 when variation in CO_2 fluxes was overestimated (Table 1). Values for coefficients of determination (R^2) and root mean squares for differences between modelled and EC fluxes (RMSD) were ca. 0.7 ($P < 0.0001$) and $2 \mu\text{mol m}^{-2} \text{ s}^{-1}$. Much of the unexplained variance in EC fluxes could be attributed to a random error of ca. 20 % in EC methodology (Wesely and Hart, 1985). This attribution was corroborated by root mean squares for error (RMSE) for EC measurements at LC calculated from Richardson et al. (2006) that were similar to RMSD, indicating that further constraint in model testing could not be achieved without further precision in EC measurements.

Table 1. Statistics from regressions of simulated on measured (a , b), and measured on simulated (R^2 , RMSD), hourly CO₂ fluxes over a boreal fen at Lost Creek, WI. All measured values were recorded at $u > 0.2 \text{ m s}^{-1}$.

	n	a^\dagger $\mu\text{mol m}^{-2} \text{ s}^{-1}$	b^\ddagger	R^2^\ddagger	RMSD ‡ $\mu\text{mol m}^{-2} \text{ s}^{-1}$	RMSE § $\mu\text{mol m}^{-2} \text{ s}^{-1}$
2001	6366	0.0	0.94	0.65	2.1	2.2
2002	6796	0.0	1.05	0.75	1.9	2.1
2003	5509	-0.1	0.96	0.72	2.2	2.5
2004	4695	-0.2	1.22	0.73	1.5	2.2
2005	4251	0.1	0.98	0.72	2.7	2.5
2006	4576	0.1	1.06	0.73	2.5	2.4

$^\dagger Y = a + bX$ from regression of simulated Y on measured X .

$^\ddagger R^2$ = coefficient of determination and RMSD = root mean square for difference from regression of measured Y on simulated X .

§ RMSE = root mean square for error of measured fluxes calculated from Richardson et al. (2006).

3.2 Water table and seasonal net ecosystem productivity

The water table measured at Lost Creek from 2001 to 2006 typically remained within 0.2 m of hummock surfaces until May, but descended to depths varying from 0.4 to 0.7 m during July through September before rising gradually thereafter (Fig. 2). These seasonal trends in WTD were simulated from transfers of water in vertical [B1] and lateral [D1, D10] directions through surface and subsurface boundaries (Fig. 1) as described in Sect. 2.1 above. WTD in the model was close to that measured in unfrozen soil during most years, but remained lower than that measured in unfrozen soil during 2001 and 2003, and in frozen soil during most years of the study (Fig. 2). The greater WTD modelled in frozen soil was attributed to slow subsurface recharge of soil water drawn to near-surface freezing zones with lower ψ_s .

Net ecosystem productivity (NEP), calculated from daily sums of gap-filled EC fluxes at Lost Creek from 2001 through 2006, remained negative (net C emissions) until warming in May, rose rapidly during late May and June to reach $2\text{--}4 \text{ g C m}^{-2} \text{ d}^{-1}$ (net C uptake) during late June and July, then declined gradually during August, becoming negative again after late September (Fig. 2). These seasonal trends in NEP were modelled from changes in net CO₂ exchange driven by those in GPP [C1], R_a [C13] and R_h [A11] with changes in weather and hydrology, as described in Sect. 2.1 above. Because CO₂ fluxes in the model were consistent with those measured by EC (Table 1), net C uptake modelled during growing seasons was similar to that calculated from gap-filled EC. However, net C emissions modelled during late spring and early autumn were consistently larger than those calculated from gap-filled EC.

3.3 Water table and diurnal CO₂ exchange

Changes in WTD were found to have contrasting effects on ecosystem CO₂ exchange, depending on the WTD at which changes occurred. To investigate relationships between WTD and ecosystem CO₂ exchange, diurnal CO₂ fluxes were examined during selected intervals with different WTD and

weather in 2002 and 2006, when seasonal WTD was shallowest and deepest, respectively, during the study period (Fig. 2e, q).

These fluxes were first examined during mid-May 2002 vs. 2006 when the water table was shallowest (Fig. 2e, q) and the weather was cool (Fig. 3a, d). Only very low CO₂ influxes and effluxes were modelled and measured in 2002 (Fig. 3c) when the water table was near the surface (Fig. 2e). Larger CO₂ influxes and effluxes were modelled and to a lesser extent measured under comparable weather (similar range of radiation and temperature in Fig. 3a, d) in 2006 (Fig. 3f) when the water table was about 0.2 m below the surface (Fig. 2q). In both years, low LE effluxes modelled and measured during May delayed soil drying and water table decline.

CO₂ fluxes were then examined during mid-August 2002 vs. 2006 when WTD and weather were near respective seasonal averages (Fig. 4). CO₂ effluxes modelled over a WTD just below 0.2 m in 2002 (Fig. 2e) were slightly less than those modelled under comparable weather conditions (similar radiation and temperature in Fig. 4a, d) over a WTD of 0.7 m in 2006 (Fig. 2q) (-4 vs. $-5 \mu\text{mol m}^{-2} \text{ s}^{-1}$ in Fig. 4c vs. f). Peak CO₂ influxes modelled over the shallower water table in 2002 were slightly smaller than those over the deeper water table in 2006 (13 vs. $14 \mu\text{mol m}^{-2} \text{ s}^{-1}$ in Fig. 4c vs. f), even though greater effluxes of LE vs. H indicated better hydration in 2002 (Fig. 4b vs. e). In both years CO₂ influxes and effluxes modelled over hollows were smaller than those over hummocks (Fig. 4c, f) because the hollow surface was 0.075 m closer to the water table of the interconnected hummock and hollow (Fig. 1). However, these small differences in CO₂ fluxes modelled with landscape position or WTD could not be clearly resolved in the EC measurements.

CO₂ fluxes were then examined during late June–early July 2002 vs. 2006 when different WTD under comparable warming events (Fig. 5a, d) enabled interactive effects of WTD and temperature on CO₂ exchange to be investigated (Fig. 5c, f). Warming in 2002 over a WTD just above 0.2 m (Fig. 2e) caused rises in LE but not in H (Fig. 5b), indicating that the fen surface remained well hydrated. Warming also caused sharp rises in CO₂ effluxes and only slight declines CO₂ influxes (Fig. 5c), indicating that both respiration and productivity, estimated from differences between diurnal influxes and effluxes, rose with warming over a shallower water table. However, the same warming in 2006 over a WTD of ca. 0.7 m (Fig. 2q) during a dry period (Fig. 2p) caused much smaller rises in LE, and larger rises in H (Fig. 5e), indicating some drying of the fen surface. In both years, Bowen ratios ($\beta = H/LE$) declined as LE rose with warming at hourly and daily time scales, but remained consistently larger in 2006 vs. 2002 (Fig. 6b vs. a), indicating constraints on LE imposed by soil drying over the deeper water table. Warming in 2006 caused much smaller rises in CO₂ effluxes, but sharper declines in CO₂ influxes than did similar warming in 2002 (Fig. 5f), indicating that both

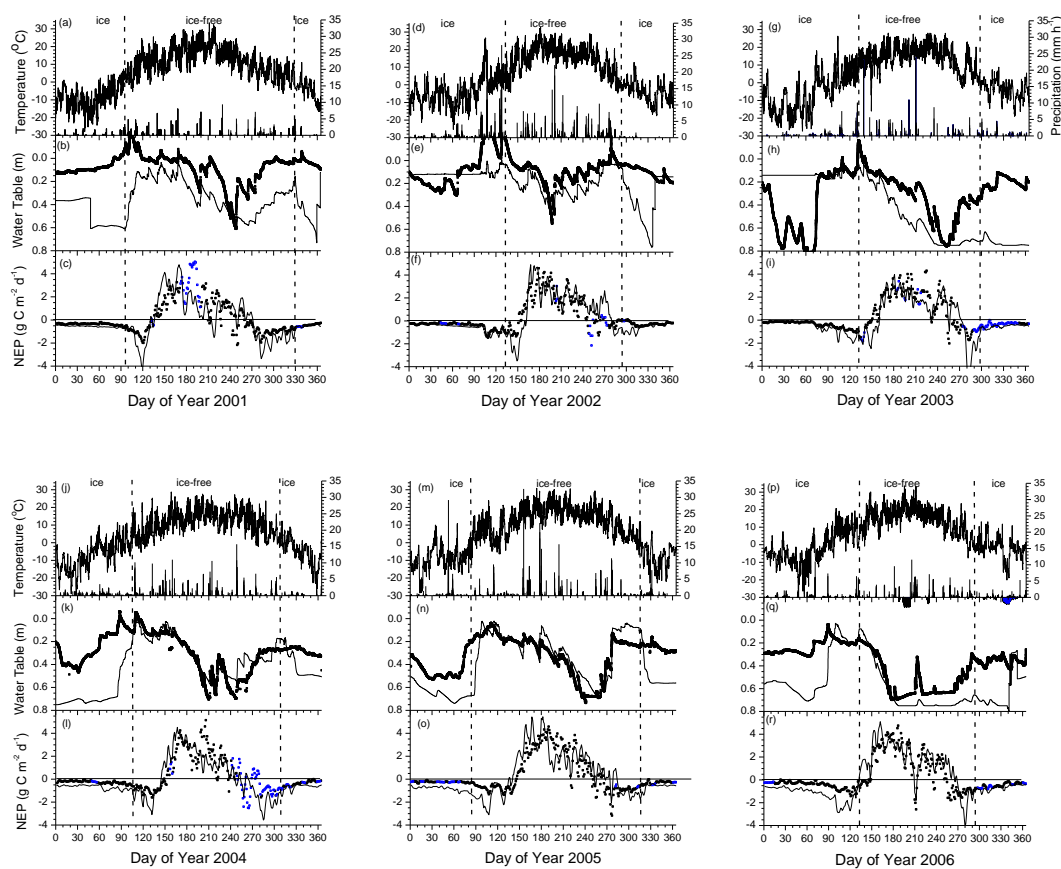


Fig. 2. Hourly air temperatures and precipitation, water table depth and net ecosystem productivity measured (symbols) and modelled (lines) from 2001 to 2006 at Lost Creek, WI. Open symbols represent daily totals calculated from more than 24 gap-filled 1/2-hourly values.

respiration and productivity were constrained by soil drying during warming over a deeper water table. Thus, CO_2 exchange responded differently to a lower water table under warmer weather, which induced surface drying (Fig. 5), than under cooler weather, which did not (Figs. 3 and 4). The constraint of surface drying on R_h was later alleviated by several precipitation events (Fig. 7a) that raised effluxes of LE vs. H (Fig. 7b), and sharply raised effluxes of CO_2 , causing a brief but pronounced decline in NEP (Fig. 2f).

The effects of WTD on CO_2 effluxes in Figs. 3–5 were modelled through the effects of WTD on $[\text{O}_{2s}]$. The near-surface water table in May 2002 (Fig. 2e) caused $[\text{O}_{2s}]$ in the model to decline sharply with depth under hummocks and hollows (Fig. 8a), thereby strongly limiting C oxidation and hence CO_2 effluxes (Fig. 3c). The slightly deeper water table in May 2006 (Fig. 2q) caused $[\text{O}_{2s}]$ to decline slightly less sharply with depth, partially alleviating O_2 limitation to C oxidation (Fig. 3f). Deepening water tables in summer 2002 allowed $[\text{O}_{2s}]$ to decline less sharply with depth than in May (Fig. 8b, c), enabling more rapid C oxidation (Figs. 4c and 5c). The very deep water tables in summer 2006 (Fig. 2q) allowed $[\text{O}_{2s}]$ to remain close to atmospheric equivalents through most of the rooting zone (Fig. 8b,c), largely alleviat-

ing O_2 limitation to C oxidation (Figs. 4f and 5f). The sharp declines in $[\text{O}_{2s}]$ in the model occurred at depths which corresponded to those of the water table (Fig. 2), indicating the effectiveness of saturated soil in reducing O_2 concentrations.

3.4 Water table and annual C balances

Annual totals of GPP, R_a , NPP and R_h modelled over hummocks and hollows exhibited interannual variability associated with mean annual temperature (MAT), precipitation, WTD and landscape position (Table 2). Annual NPP modelled in 2001 gave peak above-ground phytomasses for shrubs and sedges averaged for hummocks and hollows of 401 and 110 g C m^{-2} , comparable to ones of 414 and 79 g C m^{-2} (assuming 50% C in DM) reported in Sulman et al. (2009). Losses of CH_4 and of dissolved organic and inorganic C (DOC and DIC) also varied with MAT, precipitation, WTD and landscape position (Table 2), and caused net ecosystem C balance ($\text{NECB} = \text{NEP} - \text{CH}_4 - \text{DOC} - \text{DIC}$) to be 15–25% less than NEP. Although greater WTD in 2006 vs. 2002 caused diurnal CO_2 influxes both to increase (Figs. 3 and 4) and decrease (Fig. 5), depending on WTD and weather, at an annual time scale variation in GPP

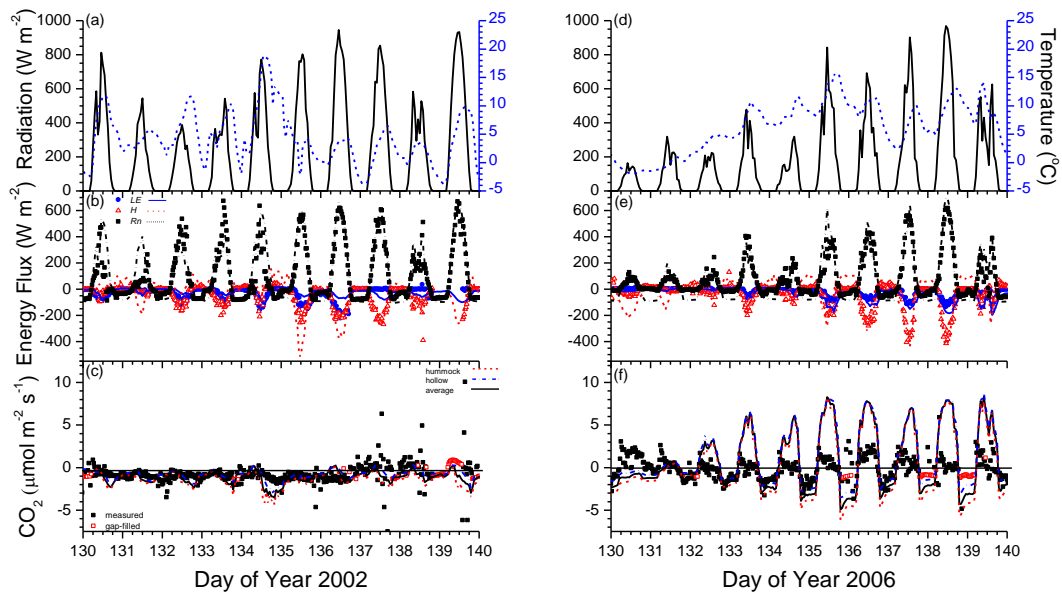


Fig. 3. Radiation and air temperature, energy and CO_2 fluxes measured (symbols) and modelled (lines) from DOY 131 to 140 with high water table in 2002 (0.0 m in Fig. 2) and lower water table in 2006 (0.2 m in Fig. 2). Positive values represent downward fluxes, negative values represent upward fluxes.

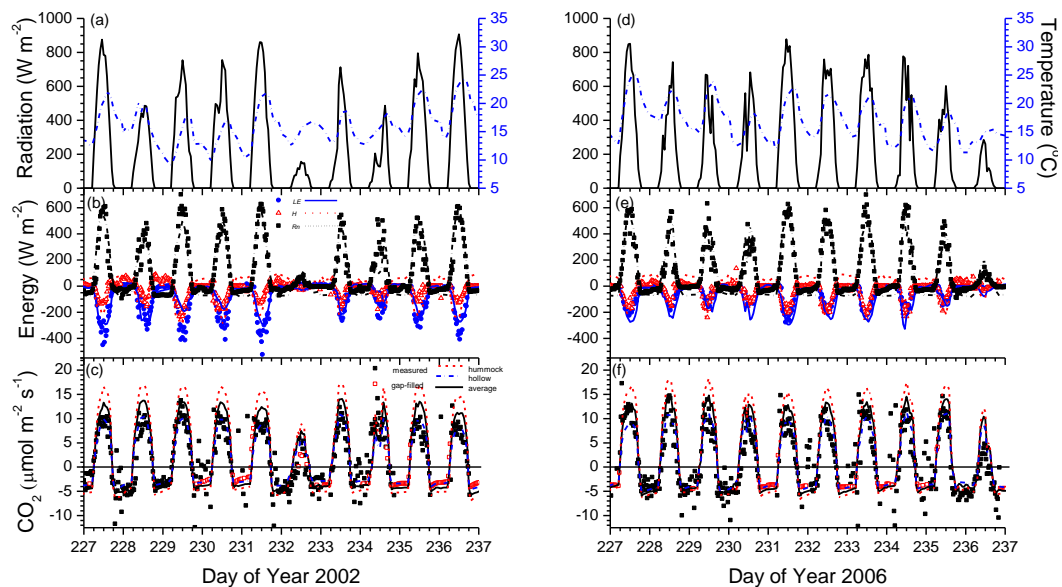


Fig. 4. Radiation and air temperature, energy and CO_2 fluxes measured (symbols) and modelled (lines) from DOY 228 to 237 with high water table in 2002 (0.2 m in Fig. 2) and low water table in 2006 (0.7 m in Fig. 2). Positive values represent downward fluxes, negative values represent upward fluxes.

and NPP appeared to be driven more by variation in MAT (R^2 for NPP vs. MAT = 0.91) than in WTD (R^2 for NPP vs. WTD = 0.05). Thus, GPP and NPP declined with MAT from 2001 to 2003 and rose with MAT from 2004 to 2006 (Table 2), as has been modelled and measured at several boreal sites in North America during this period (Grant et al., 2009a, b; Krishnan et al., 2008).

However, variation in annual R_h appeared to be driven more by variation in WTD (R^2 for R_h vs. WTD = 0.31) than in MAT (R^2 for R_h vs. MAT = 0.07) (Table 2). Greater WTD in 2006 vs. 2002 caused diurnal CO_2 effluxes driven largely by R_h to increase under seasonally average weather (Figs. 3 and 4) and to decrease under warmer weather (Fig. 5). However, these decreases in CO_2 effluxes were modelled

infrequently so that at an annual time scale the shallower water table in 2002 reduced R_h and the deeper water tables thereafter increased R_h (Table 2). Consequently, annual NECB in the model was greatest in 2002 with the shallowest water table and hence lowest R_h , and smallest in 2004 with the lowest MAT and hence NPP.

Landscape position had a large effect on ecosystem productivity in the model. Greater annual GPP, R_a , R_h and hence NECB were modelled over greater WTD in hummocks vs. hollows (Table 2), driven by greater diurnal CO_2 fluxes (Figs. 3, 4, 5). The greater GPP was attributed to improved nutrient status in hummocks, apparent as greater foliar N contents in Table 2. This improved nutrient status allowed greater dominance of shrub over sedge, apparent as greater GPP and NPP ratios, to be modelled in hummocks than in hollows (Table 2). Greater effluxes of CH_4 , DOC and DIC were modelled in years with greater precipitation and shallower water tables such as 2002, and from hollows vs. hummocks in all years of the study (Table 2).

3.5 Sensitivity of CO_2 exchange to water table

The responses of CO_2 exchange to seasonal and interannual changes in WTD (Figs. 1–7) determined those to long-term changes in WTD caused by raising or lowering the external water table. Raising the external water table by 0.3 m slowed discharge and hastened recharge through the lateral boundaries of the modelled landscape (Fig. 1), and thereby raised the internal water table from that in the earlier model run (Fig. 9a, c). Conversely, lowering the external water table by 0.3 m hastened discharge and slowed recharge, and thereby lowered the internal water table. Subsidence of the fen surface with drainage was not modelled, so that WTD in these runs referred to an unchanged surface elevation. These changes in WTD had contrasting effects on NEP modelled at different times of the year in 2002 and 2006. In 2002, lowering the water table decreased NEP until the end of June, increased it slightly during July and early August, but decreased it again thereafter (Fig. 9b). In 2006, lowering the water table decreased NEP until the end of May, but increased NEP thereafter (Fig. 9d). In general, lowering the water table reduced NEP when the WTD was less than ca. 0.2 m, and increased NEP when it was greater.

A transition from increases to decreases in NEP with deeper water tables occurred in late August 2002 (Fig. 9b). The cause of this transition was investigated by examining the diurnal CO_2 exchange modelled during the period in which the transition occurred (Fig. 10). Lowering the water table (Fig. 10a) increased daytime near-surface soil temperatures (Fig. 10b) and both influxes and effluxes of CO_2 (Fig. 10c). Precipitation on DOY 232 (Fig. 2d) raised all water tables by ca. 0.1 m, so that the shallowest water table rose above 0.2 m (Fig. 10a). This rise caused CO_2 effluxes to decrease, and consequently CO_2 influxes to increase, over the shallower water table with respect to those over the deeper

(Fig. 10c). These decreased effluxes were modelled from lower $[\text{O}_{2s}]$ in a shallower aerobic zone following the rise in water table (Fig. 11b vs. a). These changes in CO_2 effluxes vs. influxes with WTD caused the transition from increases to decreases in NEP with deeper water tables in late August 2002 (Fig. 9b). Lowering the much deeper water table during the same period in 2006 (Fig. 10d) had little effect on near-surface soil temperatures (Fig. 10e) or on CO_2 effluxes (Fig. 10e), but increased CO_2 influxes and hence NEP (Fig. 9d).

3.6 Sensitivity of annual C balances to watertable

Responses of NEP to changes in WTD at seasonal (Fig. 9) and diurnal (Fig. 10) time scales were aggregated to the annual time scale for 2001 to 2006 in Table 3. Lowering the water table increased GPP and NPP of shrub, and to a lesser extent of sedge, in each year of the study. Lowering the water table also increased R_h in each year of the study, but more in years with shallow water tables such as 2002 (as in Fig. 10c) and less in years with deeper water tables such as 2006 (as in Fig. 10f). These increases in R_h were greater than those in NPP when WTD was small, so that lowering the water table reduced NECB during 2002 (as in Fig. 9b). However, these increases in R_h were less than those in NPP when WTD was large so that lowering the water table increased NECB during 2006 (as in Fig. 9d). Increases in R_h were similar to those in NPP during years with intermediate WTD, so that lowering the water table had smaller effects on NECB during the other years of the study. Lowering the water table also decreased CH_4 emissions, particularly during 2002 (Table 3).

4 Discussion

4.1 Model processes by which WTD affects CO_2 exchange

The modelling of WTD effects on peatland CO_2 exchange in *ecosys* is based on the explicit coupling of oxidation–reduction reactions which drive C and N transformations in soil, roots and mycorrhizae with gaseous and aqueous transfers of the substrates and products of these reactions through soil and root profiles with dynamic WTD. This coupling allowed the model to simulate complex responses of CO_2 exchange to changes in WTD. The processes by which this simulation was accomplished are described below.

4.1.1 CO_2 effluxes and WTD

Rates of C oxidation and hence of CO_2 effluxes by microbial, root and mycorrhizal populations in *ecosys* were governed by their rates of O_2 reduction [A14, C14b]. These rates were in turn governed by $[\text{O}_{2s}]$ [A17a, b, C14c, d] determined by convective and dispersive transport from the atmosphere through gaseous [D16a–d] and aqueous [D19] phases in soil

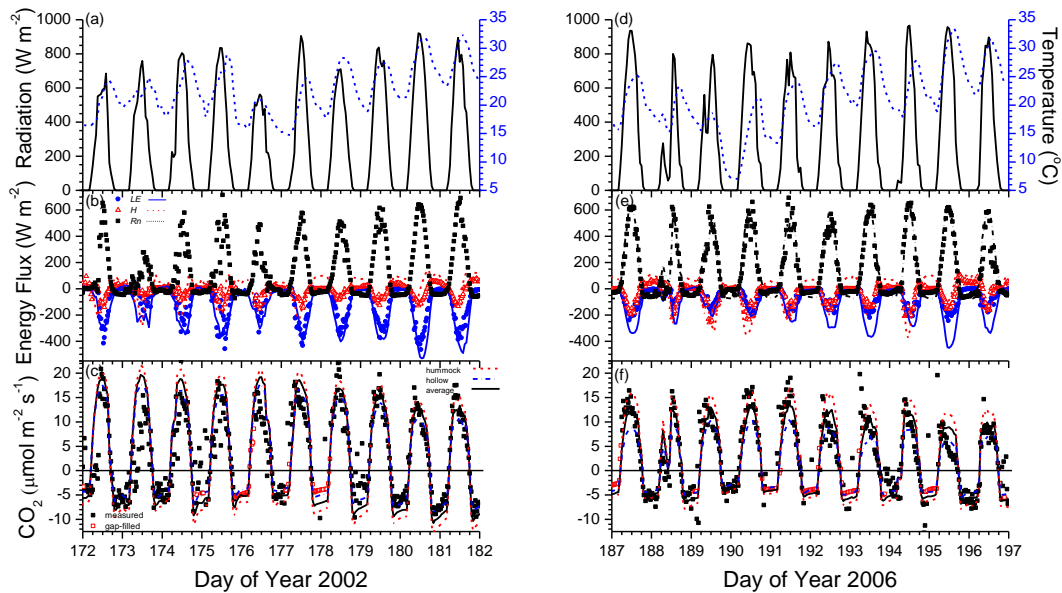


Fig. 5. Radiation and air temperature, energy and CO₂ fluxes measured (symbols) and modelled (lines) during warming events with high water table from DOY 173 to 182 in 2002 (0.2 m in Fig. 2) and low water table from DOY 188 to 197 in 2006 (0.7 m in Fig. 2). Positive values represent downward fluxes, negative values represent upward fluxes.

Table 2. Landscape position, mean annual temperature (MAT), total precipitation, average WTD from hummock surface between DOY 120 and 300 (modelled/measured), foliar N content at anthesis, gross primary productivity (GPP), autotrophic respiration (R_a), net primary productivity (NPP), heterotrophic respiration (R_h), methane emissions (CH₄), export of dissolved organic and inorganic C (DOC + DIC), net ecosystem carbon balance (NECB = NEP – CH₄ – DOC – DIC) and net ecosystem productivity (NEP = NPP – R_h) modelled and derived from eddy covariance (EC) measurements for a boreal fen at Lost Creek, WI. Positive values for NECB and NEP represent C gains, negative values C losses. Average values are simple means of those for interconnected hummocks and hollows.

Year	Position	MAT	Precip. mm yr ⁻¹	Water Table mod./mes. m	Foliar N shrub/sedge g N kg C ⁻¹	GPP shrub/sedge	R_a shrub/sedge	NPP shrub/sedge	R_h	CH ₄	DOC + DIC	NECB	NEP mod./EC
		°C											
2001	hummock				27/28	1136/171	493/080	643/091	722	2.9	0	9	
	hollow				20/24	494/374	226/167	268/207	532	5.4	15	-77	
	average	5.6	865	0.33/0.12	23/26	815/273	360/124	456/149	627	4.2	8	-34	-22/+63
2002	hummock				32/34	1064/153	465/074	599/079	599	3.3	-2	79	
	hollow				23/32	521/383	231/187	290/196	395	3.8	26	61	
	average	4.9	965	0.17/0.07	28/33	793/268	348/131	445/138	497	3.6	12	70	+86/+96
2003	hummock				32/29	1017/146	446/063	571/083	650	1.7	-1	4	
	hollow				22/31	479/380	227/177	252/203	489	2.1	9	-45	
	average	4.1	692	0.49/0.31	27/30	748/263	337/120	411/143	570	1.9	4	-21	-16/+94
2004	hummock				27/24	972/125	404/052	568/073	683	0.8	0	-43	
	hollow				21/26	482/362	207/154	275/208	520	1.1	15	-53	
	average	4.0	814	0.32/0.35	24/25	727/244	306/103	421/141	602	1.0	8	-48	-40/+67
2005	hummock				31/25	1231/142	547/066	684/076	654	2.1	0	103	
	hollow				22/29	554/403	251/187	303/216	497	2.8	18	1	
	average	5.7	790	0.30/0.35	27/27	893/273	399/127	494/146	576	2.5	9	52	+64/+102
2006	hummock				30/24	1174/136	503/060	671/076	695	2.0	-3	52	
	hollow				22/27	587/388	263/178	324/210	525	2.1	9	-2	
	average	6.1	665	0.60/0.49	26/26	881/262	383/119	498/143	610	2.1	3	25	+31/+79

and roots, by dissolution from gaseous to aqueous phases in soil and roots [D14a, b], and by diffusion to and uptake at microbial [A17a, b], root and mycorrhizal [C14c, d] surfaces. Above the water table, [O_{2s}] calculated from these equations was well above the Michaelis-Menten constant used for microbial, root and mycorrhizal uptake (0.064 g O₂ m⁻³ in [A17a] and [C14c]) (Figs. 8, 11), so that C oxidation was

not much limited by O₂ reduction. Below the water table, [O_{2s}] declined sharply to values that were two orders of magnitude smaller than this constant, so that C oxidation was strongly limited by O₂ reduction. Although C oxidation in *ecosys* was also coupled with reduction of DOC by anaerobic heterotrophic fermenters, generating CO₂, H₂ and acetate that drives heterotrophic and autotrophic CH₄ production

Table 3. External WTD, mean annual temperature (MAT), total precipitation, average WTD from hummock surface between DOY 120 and 300, foliar N content at anthesis, gross primary productivity (GPP), autotrophic respiration (R_a), net primary productivity (NPP), heterotrophic respiration (R_h), methane emissions (CH_4), export of dissolved organic and inorganic C (DOC + DIC), and net ecosystem carbon balance (NECB = $\text{NEP} - \text{CH}_4 - \text{DOC} - \text{DIC}$), averaged for hummock and hollow landscape positions, modelled for a boreal fen at Lost Creek, WI. Values at 0.60 m in bold are the same as those in Table 2.

Year	External Water Table	MAT	Precip.	Water Table	Foliar N shrub/sedge	GPP shrub/sedge	R_a shrub/sedge	NPP shrub/sedge	R_h	CH_4	DOC + DIC	NECB
	m											
2001	0.30	5.6	865	0.25	22/26	762/279	338/125	424/154	580	6.8	8	-17
	0.60			0.33	23/26	815/273	360/124	456/149	627	4.2	8	-34
	0.90			0.45	25/27	861/299	377/137	484/162	660	2.0	9	-25
2002	0.30	4.9	965	0.14	26/33	760/263	336/127	424/136	426	7.2	18	109
	0.60			0.17	28/33	793/268	348/131	445/138	497	3.6	12	70
	0.90			0.33	30/35	832/295	366/142	466/153	570	1.9	12	36
2003	0.30	4.1	692	0.43	24/29	717/252	328/119	389/133	538	4.4	7	-27
	0.60			0.49	27/30	748/263	337/120	411/143	570	1.9	4	-21
	0.90			0.73	30/29	822/282	359/124	463/158	591	0.6	1	27
2004	0.30	4.0	814	0.26	22/25	690/238	297/102	393/136	557	1.3	8	-36
	0.60			0.32	24/25	727/244	306/103	421/141	602	1.0	8	-48
	0.90			0.36	25/25	768/247	317/105	451/142	656	0.6	5	-68
2005	0.30	5.7	790	0.21	25/27	793/249	362/114	431/135	507	3.8	7	48
	0.60			0.30	27/27	893/273	399/127	494/146	576	2.5	9	52
	0.90			0.36	29/27	938/276	416/129	522/147	627	1.8	8	32
2006	0.30	6.1	665	0.57	24/25	784/257	352/121	432/136	564	2.7	1	0
	0.60			0.60	26/26	881/262	383/119	498/143	610	2.1	3	25
	0.90			0.74	29/27	925/285	396/131	529/154	620	1.6	5	56

(Grant, 1998) (Tables 2, 3), the energy yield from reduction of DOC was much smaller than that of O_2 (Brock and Madigan, 1991), and so drove slower microbial growth [A21] and hence C oxidation [A13].

Under the site conditions presented to the model in this study, $[\text{O}_{2s}]$ above the Michaelis-Menten constant to a depth of ca. 0.2 m (e.g. Fig. 8b) was sufficient to sustain rapid rates of C oxidation and hence CO_2 effluxes (e.g. Fig. 5c). Shallower aerobic zones (e.g. Fig. 8a) reduced CO_2 effluxes (e.g. Fig. 3c vs. f), while deeper aerobic zones (e.g. Fig. 8c) increased CO_2 effluxes only slightly (Fig. 4f vs. c). Deeper water tables also raised soil temperatures [D12] (Fig. 10b) by reducing water contents, further contributing to increases in rates of C oxidation through Arrhenius functions for R_h [A6] and R_a [C22a, b]. These model processes thus enabled the simulation of greater CO_2 effluxes over deeper water tables vs. smaller effluxes over shallower, particularly within the upper 0.2 m of the soil profile, consistent with greater effluxes measured with greater WTD at Lost Creek (Sulman et al., 2009) and elsewhere (e.g. Moore and Dalva, 1993; Moore and Roulet, 1993; Silvola et al., 1996). The model processes were also able to simulate greater R_h and hence greater CO_2 effluxes, as well as smaller CH_4 effluxes, over greater WTD in hummocks vs. hollows (Figs. 3, 4, 5; Table 2), as has been reported from field sites (Strack and Waddington, 2007).

However, smaller CO_2 effluxes were modelled and measured over deeper water tables (Fig. 5f vs. c) during periods

of high temperature (Fig. 5d) and low precipitation (Fig. 2p) when drying, evidenced by higher Bowen ratios (Fig. 6), limited C oxidation in surface soil and litter (Fig. 7c). Drying of surface soil and litter was modelled when capillary rise of water [D7] plus diffusive transfer of vapor [D16] from wetter soil below failed to replace evaporative transfer of vapor to the atmosphere above [D6]. Surface drying therefore depended on soil and hydraulic properties (Fig. 1) as well as on weather. Limitations to C oxidation caused by drying were modelled from functions for competitive inhibition of heterotrophic decomposers exacerbated by low water content [A3, A5], and for constraints to microbial growth from low water potentials [A15], which together slowed R_h in dry soil and litter (Grant et al., 2012). These limitations were rapidly alleviated by rainfall and consequent surface wetting (Fig. 7), enabling the simulation of CO_2 emission pulses commonly observed after rainfall on dry soil (Huxman et al., 2004).

These model processes thus enabled the simulation of smaller CO_2 effluxes sometimes measured over deeper water tables. By simulating rises in CO_2 effluxes when shallower water tables were lowered (Fig. 10c), and no change or declines in CO_2 effluxes when deeper water tables were lowered (Fig. 10f), the model explained apparently contradictory increases, no changes, and decreases of soil respiration that have been observed with increases in WTD (e.g. Lafleur et al., 2005a; Silvola et al., 1996). This model explanation was accomplished without arbitrary parameterizations of aerobic

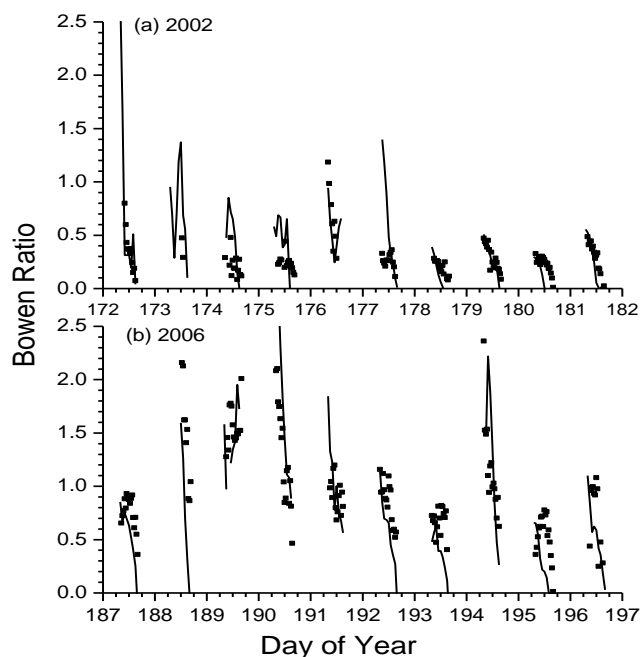


Fig. 6. Bowen Ratios measured (symbols) and modelled (lines) during warming events with high water table from DOY 173 to 182 in 2002 (0.2 m in Fig. 2) and low water table from DOY 188 to 197 in 2006 (0.7 m in Fig. 2) when net radiation $> 250 \text{ W m}^{-2}$.

vs. anaerobic respiration used in other wetland models (e.g. Clymo, 1992; St-Hilaire et al., 2010). The complex response to WTD of respiration in *ecosys* was also demonstrated by Dimitrov et al. (2010a) in an ombrotrophic bog with very different hydrologic characteristics to those of the fen at Lost Creek.

4.1.2 CO₂ influxes and WTD

The effects of WTD on CO₂ influxes were driven in large part by those on CO₂ effluxes. Over deeper water tables, increases in [O_{2s}] (e.g. Fig. 8a) raised rates of C oxidation by microbial populations [A13, A14] which drove more rapid microbial growth [A25] and hence nutrient mineralization [A26]. Increases in [O_{2s}] also raised rates of C oxidation by root and mycorrhizal populations [C14a, b], which drove more rapid root and mycorrhizal growth [C20b] and hence nutrient uptake [C23]. Greater rates of nutrient uptake increased foliar nutrient contents [C12] (Tables 2 and 3) and hence increased rates of CO₂ fixation [C6a, C7, C11]. These greater uptake rates were consistent with the experimental findings of Laiho et al. (2003) that N uptake by vascular plants was more rapid in drained vs. undrained boreal peatlands. These model processes enabled greater CO₂ influxes and hence greater NPP to be simulated over deeper vs. shallower water tables, consistent with greater influxes and NPP measured

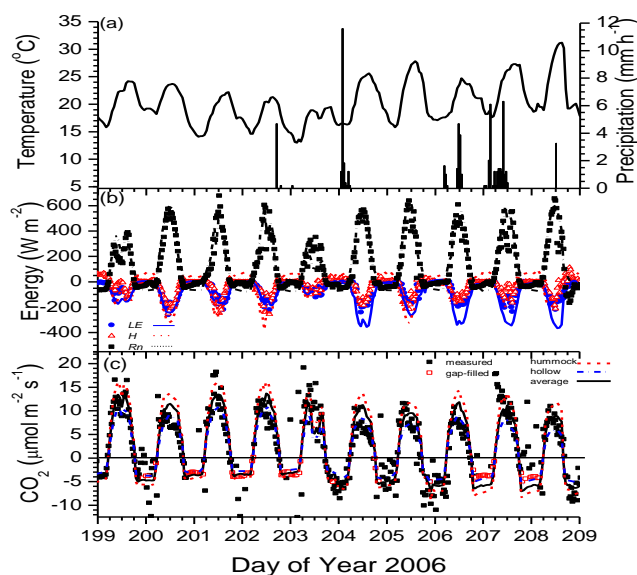


Fig. 7. Air temperature and precipitation, and energy and CO₂ fluxes measured (symbols) and modelled (lines) before and after precipitation events with a low water table from DOY 200 to 209 in 2006 (0.7 m in Fig. 2). Positive values represent downward fluxes, negative values represent upward fluxes.

with greater WTD at Lost Creek (Sulman et al., 2009) (e.g. Fig. 3f vs. 3c; Table 2). These processes also enabled the simulation of greater CO₂ influxes and hence greater NPP with greater WTD in hummocks vs. hollows (Figs. 3, 4, 5; Table 2), as has been reported from field sites (Strack and Waddington, 2007). This simulation was accomplished without arbitrary parameterizations of productivity under aerobic vs. anaerobic conditions used in other wetland models (e.g. Bond-Lamberty et al., 2007; Sonnentag et al., 2008).

However, smaller CO₂ influxes were sometimes modelled and measured over deeper water tables (Fig. 5f vs. c) under high temperature (Fig. 5d) and surface drying (Fig. 6), as was also measured in a boreal peatland by Shurpali et al. (1995). These smaller influxes were modelled from coupled processes for root water uptake [B6] and canopy transpiration [B1] that lowered canopy water potential [B14], conductance [B2] and hence CO₂ fixation [C2, C6a, C7] as soil water potentials declined with drying when upward water movement from the saturated soil zone [D7, D16] failed to maintain near-surface water contents (Grant et al., 2012). Similar declines in CO₂ influxes measured by EC and modelled by *ecosys* over greater WTD in an ombrotrophic bog were also attributed by Dimitrov et al. (2011) to water stress in moss caused by near-surface soil drying. Corresponding declines in CO₂ influxes have also been measured at WTDs below 0.2–0.5 m in a boreal fen by Sonnentag et al. (2010). The warm, dry weather and deeper water tables during which

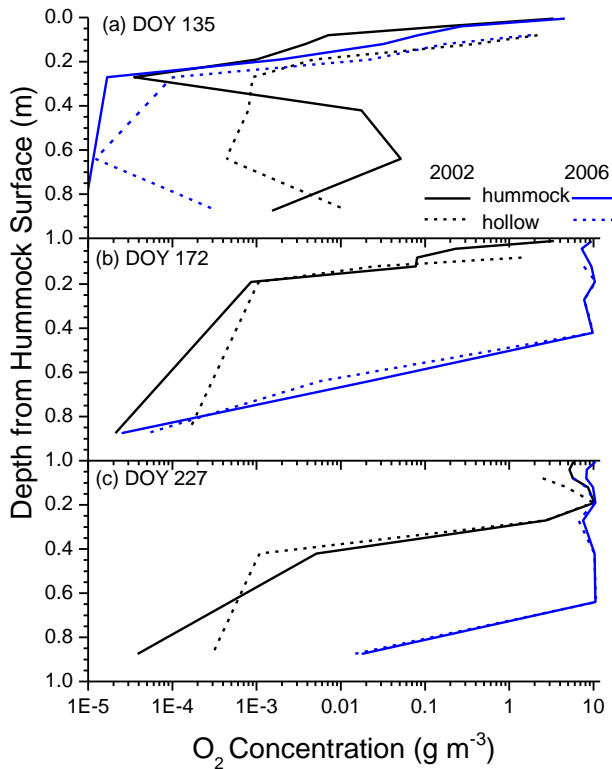


Fig. 8. Vertical profiles of aqueous O₂ concentration ([O_{2s}]) modelled below hummocks and hollows on DOY 172 and 227 of 2002 and 2006.

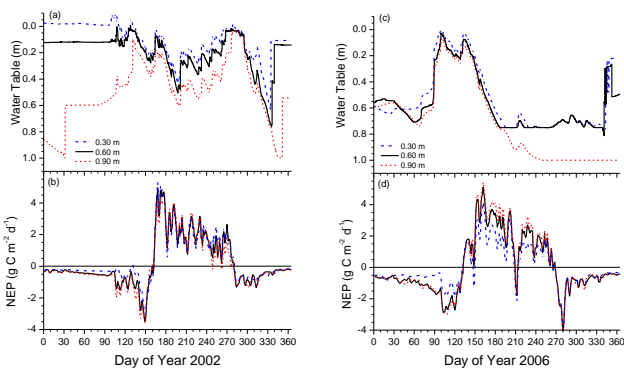


Fig. 9. Changes in water table depth and net ecosystem productivity (NEP) modelled by raising or lowering the depth of the external water table from 0.6 m (Fig. 1) to 0.3 m or 0.9 m in 2002 and 2006. WTD and NEP modelled at 0.6 m are the same as those in Fig. 2.

these smaller influxes were modelled did not occur frequently enough at Lost Creek to lower annual GPP and NPP, both of which rose with deeper water tables in all years of the study (Tables 2 and 3). However, if warming events over deeper water tables were to occur more frequently under proposed climate change, these adverse effects on annual GPP and NPP might become more apparent.

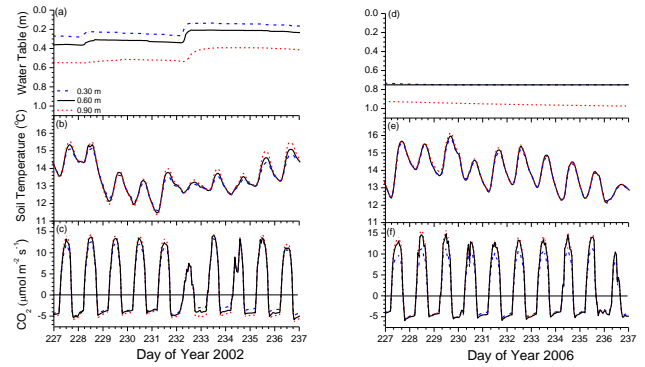


Fig. 10. Changes in water table depth, soil temperatures at 0.12 m, and CO₂ fluxes modelled from DOY 228 to 237 in 2002 and 2006 by raising or lowering the depth of the external water table from 0.6 m (Fig. 1) to 0.3 m or 0.9 m. CO₂ fluxes modelled at 0.6 m are the same as those in Fig. 4.

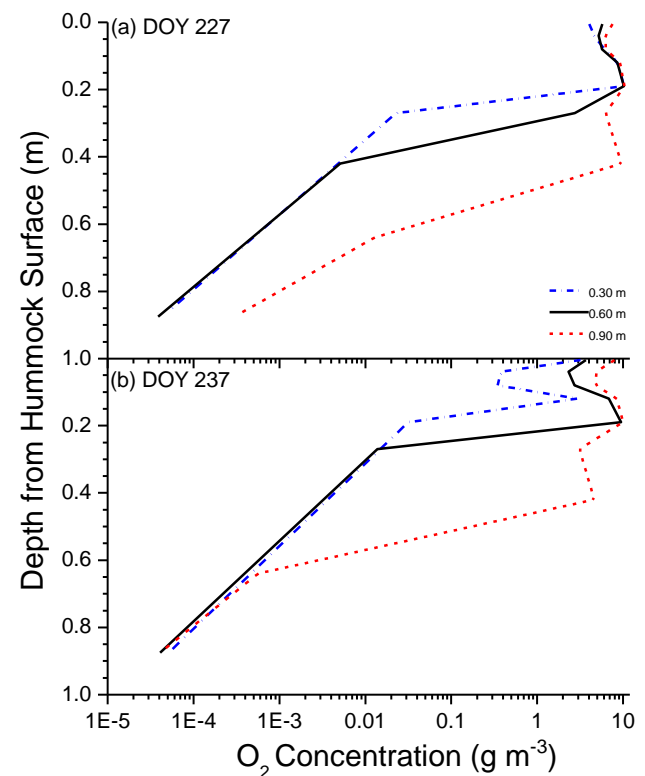


Fig. 11. Vertical profiles of aqueous O₂ concentration ([O_{2s}]) modelled below hummocks by raising or lowering the depth of the external water table from 0.6 m (Fig. 1) to 0.3 m or 0.9 m on DOY 227 and 237 in 2002.

4.1.3 Net CO₂ exchange and WTD

The combined effects of WTD on CO₂ effluxes and influxes caused greater NECB to be modelled in a cooler year with shallower water table such as 2002 than in a warmer year with a deeper one such as 2006 (Table 2). However, the

lowest NECB in this study was modelled in 2004 with an average WTD but the lowest MAT, so that annual NECB was better correlated with MAT than with annual average WTD, as found elsewhere by Lafleur et al. (2005). Sulman et al. (2009) calculated slightly greater NEP in 2002 than in 2006, and lower NEP in 2004, from gap-filled EC fluxes at Lost Creek (Table 2), which was consistent with model results, and so also did not find a correlation between annual WTD and NEP. However, their annual NEP was generally larger than NEP and NECB modelled here, in part because they did not account for losses as CH₄, DOC and DIC (Table 2), and in part because CO₂ effluxes measured by EC during peak emission periods in late spring and early autumn were smaller than those modelled (Fig. 2). In the model, these peaks preceded the phenologically-driven onset of CO₂ fixation in spring when CO₂ uptake failed to offset CO₂ emissions from warming and draining soils, and followed the phenologically-driven termination of CO₂ fixation in autumn when CO₂ uptake failed to offset CO₂ emissions from warmed and drained soils. Similar emission peaks of 2–3 g C m⁻² d⁻¹ were measured in a boreal fen by Joiner et al. (1999) during periods between spring thaw and the onset of CO₂ fixation, and between the termination of CO₂ fixation and autumn freezing. However, the magnitude of these peaks depended on the timing of thawing and freezing vs. that of the onset and termination of CO₂ fixation, so that interannual variation in this timing contributed to substantial differences in annual NEP and hence NECB, as modelled in this study (Fig. 2). The comparatively low annual NECB modelled here reflects the growth habit of the shrub – sedge plant functional types at Lost Creek in which there was no long-term accumulation of woody C. Correlations of annual NECB with MAT and WTD among years were complicated by the effects on R_h of changes in litter stocks carried over from previous years with differing productivity.

Differences among annual NECB with WTD in the model were consistent with experimental findings from an open peatland in nearby Minnesota over which a net C uptake of 32 g m⁻² was measured from May to October in a wet year and a net C emission of 71 g m⁻² was measured during the same period in a dry year (Shurpali et al., 1995). Differences in the model were also consistent with experimental findings from a boreal fen over which a net C uptake of 92 g m⁻² was measured in a wetter year and a net C emission of 31 g m⁻² was measured during a drier year with earlier snowmelt (Joiner et al., 1999). Contrasting changes in annual NECB modelled when water tables were lowered at smaller vs. greater WTD (e.g. 2002 vs. 2006 in Table 3) were consistent with the findings of Minkkinen et al. (2002) that peat C accumulation rates usually increase but may decrease with drainage of boreal wetlands in Finland. The contributions of DOC losses to NECB in the model (Tables 2 and 3) were similar to ones of 8–11 g C m⁻² y⁻¹ or about 17 % of NEP measured in a boreal fen by Strack et al. (2008).

4.2 Sensitivity of species composition to changes in water table

Changes in water table had different effects on CO₂ exchange by shrubs and sedges in the model. Larger root porosity θ_{pr} [D17d] used for sedges, as described in Sect. 2.2 above, enabled more rapid O₂ uptake through sedge root axes [D16d], particularly when [O_{2s}] and hence [O_{2r}] [D14] were low. Consequently, O₂ uptake [C14c] and hence C oxidation [C14b] by sedge roots were less dependent on convection-dispersion [D16a-c] and diffusion [C14d] through soil to root surfaces. Therefore GPP and NPP of sedges increased while those of shrubs decreased in hollows vs. hummocks where the water tables were shallower (Table 2). At the landscape scale, GPP and NPP of sedges declined less than did those of shrubs when water tables were raised (Table 3) and root O₂ uptake became more dependent on root O₂ transport. Conversely, productivity of sedge rose less than that of shrubs when water tables were lowered (Table 3), which was consistent with declines in graminoid biomass and increases in shrub biomass observed after lowering water tables in boreal peatlands from chronosequence studies by Laiho et al. (2003), drainage studies by Weltzin et al. (2003) and natural drying by Sonnentag et al. (2010). Thus, θ_{pr} was a key attribute for plant adaptation to wetland conditions in *ecosys*, allowing changes in species composition with changes in WTD. Such changes in composition are an important adaptive response that reduces the impact of changes in hydrology on wetland productivity. At the present stage of model development, this attribute is not dynamic, although θ_{pr} has been found to rise in anoxic soils (Visser et al., 2000).

5 Conclusions

The model was able to simulate complex responses of CO₂ exchange to changes in WTD at diurnal, seasonal and annual time scales that were consistent with those observed at LC and at similar sites elsewhere. However, these responses required the explicit modelling of key processes, particularly O₂ transport, uptake and reduction, by which CO₂ exchange is determined in wetlands, and which need to be included in models used to study wetland productivity. At the diurnal time scale the following responses were found:

1. Soil CO₂ effluxes rose with greater WTD over shallow water tables (Fig. 4) because increased [O_{2s}] (Fig. 8, 11) hastened microbial and root oxidation–reduction reactions by raising energy yields [A20]. This response required explicit modelling of coupled transport and uptake processes for O₂ through soil and roots [A17, C14, D16, D19] which were parameterized independently of the model.
2. Soil CO₂ effluxes declined with greater WTD over deeper water tables (Fig. 5) because surface drying

slowed microbial oxidation–reduction reactions [A3, A5]. This response required modelling of coupled transport [D7] and evaporation [D6] processes for water through soil and surface litter from water potential gradients determined by peat hydrologic properties.

- Soil CO₂ influxes usually rose with greater WTD (Figs. 4, 10) because more rapid microbial and root oxidation–reduction reactions from (1) drove more rapid N mineralization [A25] and uptake [C23]. This response required modelling a comprehensive set of soil and plant N transformations fully coupled to those of C.
- Soil CO₂ influxes sometimes declined with greater WTD over deeper water tables during warming events (Fig. 5) because drying soils forced lower canopy water potential [B14] and hence CO₂ fixation [C2, C6a, C7]. This response required modelling the effects on CO₂ fixation of plant water status solved from hydraulically-driven water transport along soil–plant–atmosphere water potential gradients [B14].

At the annual time scale, the combined responses (1) to (4) caused

- NECB to be greater in years with shallow water tables and smaller in years with deeper water tables (Table 2),
- NECB to decline with increases in WTD in years with shallow water tables and to rise with increases in WTD in years with deeper water tables (Table 3), indicating that deepening water tables may reduce NECB only to a certain depth, below which further deepening may not.

Supplementary material related to this article is available online at: <http://www.biogeosciences.net/9/4215/2012/bg-9-4215-2012-supplement.pdf>.

Acknowledgements. Field research was funded by DOE BER NICCR 050516Z19 and NSF BIO DEB-0845166. Computational facilities for *ecosys* were provided by the University of Alberta and by the Compute Canada high performance computing infrastructure.

Edited by: P. Stoy

References

- Adkinson, A. C., Syed, K. H., and Flanagan, L. B.: Contrasting responses of growing season ecosystem CO₂ exchange to variation in temperature and WTD in two peatlands in northern Alberta, Canada, *J. Geophys. Res.*, 116, G01004, doi:10.1029/2010JG001512, 2011.
- Blodau, C., Roulet, N. T., Heitmann, T., Stewart, H., Beer, J., Lafleur, P., and Moore, T. R.: Belowground carbon turnover in a temperate ombrotrophic bog, *Global Biogeochemical Cycles*, 21, GB1021, doi:10.1029/2005GB002659, 2007.
- Boelter, D. H.: Physical properties of peats as related to degree of decomposition. *Soil Sci. Soc. Am. Pro.*, 33, 606–609, 1969.
- Bond-Lamberty, B., Gower, S. T., and Ahl, D. E.: Improved simulation of poorly drained forests using Biome-BGC, *Tree Physiology*, 27, 703–715, 2007.
- Brock, T. D. and Madigan, M. T.: *Biology of Microorganisms* (6th Edn.) Prentice Hall, NJ, 1991.
- Clymo, R. S.: Models of peat growth, *Suo*, 43, 127–36, 1992.
- Dang, Q. L. and Liefers, V. J.: Assessment of patterns of response of tree ring growth of black spruce following peatland drainage, *Can. J. For. Res.*, 19, 924–929, 1989.
- Dimitrov, D. D., Grant, R. F., LaFleur, P. M., and Humphreys, E.: Modelling the effects of hydrology on ecosystem respiration at Mer Bleue bog, *J. Geophys. Res.-Biogeo.*, 115, G04043, doi:10.1029/2010JG001312, 2010a.
- Dimitrov, D. D., Grant, R. F., LaFleur, P. M., and Humphreys, E.: Modelling subsurface hydrology of Mer Bleue bog, *Soil Sci. Soc. Am. J.*, 74, 680–694, 2010b.
- Dimitrov, D. D., Grant, R. F., LaFleur, P. M., and Humphreys, E.: Modelling the effects of hydrology on gross primary productivity and net ecosystem productivity at Mer Bleue bog, *J. Geophys. Res.-Biogeo.*, 116, G04010, doi:10.1029/2010JG001586, 2011.
- Flanagan, L. B. and Syed, K. H.: Stimulation of both photosynthesis and respiration in response to warmer and drier conditions in a boreal peatland ecosystem, *Global Change Biology*, 17, 2271–2287, doi:10.1111/j.1365-2486.2010.02378.x, 2011.
- Frolking, S., Roulet, N. T., Moore, T. R., Lafleur, P. M., Bubier, J. L., and Crill, P. M.: Modelling the seasonal to annual carbon balance of Mer Bleue bog, Ontario, Canada, *Global Biogeochem. Cy.*, 16, doi:10.1029/2001GB001457, 2002.
- Grant, R. F.: Simulation of methanogenesis in the mathematical model *ecosys*, *Soil Biol. Biochem.*, 30, 883–896, 1998.
- Grant, R. F.: Simulation of methanotrophy in the mathematical model *ecosys*, *Soil Biol. Biochem.*, 31, 287–297, 1999.
- Grant, R. F.: Modelling topographic effects on net ecosystem productivity of boreal black spruce forests, *Tree Physiology*, 24, 1–18, 2004.
- Grant, R. F. and Roulet, N. T.: Methane efflux from boreal wetlands: theory and testing of the ecosystem model *ecosys* with chamber and tower flux measurements, *Global Biogeochem. Cy.*, 16, 1054, doi:10.1029/2001GB001702, 2002.
- Grant, R. F. and Pattey, E.: Modelling variability in N₂O emissions from fertilized agricultural fields, *Soil Biol. Biochem.*, 35, 225–243, 2003.
- Grant, R. F., Oechel, W. C., Ping, C., and Kwon, H.: Carbon balance of coastal arctic tundra under changing climate, *Glob. Change Biol.*, 9, 16–36, 2003.
- Grant, R. F., Pattey, E. M., Goddard, T. W., Kryzanowski, L. M., and Puurveen, H.: Modelling the effects of fertilizer application rate on nitrous oxide emissions from agricultural fields, *Soil Sci. Soc. Am. J.*, 70, 235–248, 2006.
- Grant, R. F., Barr, A. G., Black, T. A., Margolis, H. A., Dunn, A. L., Metsaranta, J., Wang, S., McCaughey, J. H., and Bourque, C. P.-A.: Interannual variation in net ecosystem productivity of Canadian forests as affected by regional weather patterns – a Fluxnet-

- Canada synthesis, *Agric. For. Met.*, 149, 2022–2039, 2009a.
- Grant, R. F., Margolis, H. A., Barr, A. G., Black, T. A., Dunn, A. L., Bernier, P. Y., and Bergeron, O.: Changes in net ecosystem productivity of boreal black spruce stands in response to changes in temperature at diurnal and seasonal time scales, *Tree Physiol.*, 29, 1–17, 2009b.
- Grant, R. F., Barr, A. G., Black, T. A., Margolis, H. A., McCaughey, J. H., and Trofymow, J. A.: Net ecosystem productivity of temperate and boreal forests after clearcutting – a Fluxnet-Canada synthesis, *Tellus B.*, 62B, 475–496, 2010a.
- Grant, R. F., Jassal, R. S., Black, T. A., and Brummer, C.: Changes in net CO₂ and N₂O exchange with fertilization of Douglas fir: mathematical modelling in *ecosys.*, *J. Geophys. Res.*, 115, G04009, doi:10.1029/2009JG001094, 2010b.
- Grant, R. F., Humphreys, E. R., Lafleur, P. M., and Dimitrov, D. D.: Ecological controls on net ecosystem productivity of a mesic arctic tundra under current and future climates, *J. Geophys. Res. Biogeosci.*, 116, G01031, doi:10.1029/2010JG001555, 2011.
- Grant, R. F., Baldocchi, D. D. and Ma, S.: Ecological controls on net ecosystem productivity of a Mediterranean grassland under current and future climates, *Agric. For. Meteorol.*, 152, 189–200, 2012.
- Huxman, T. E., Snyder, K. A., Tissue, D., Leffler, A. J., Ogle, K., Pockman, W. T., Sandquist, D. R., Potts, D. L., and Schwinning, S.: Precipitation pulses and carbon fluxes in semiarid and arid ecosystems, *Oecologia*, 141, 254–268, 2004.
- Joiner, D. W., Lafleur, P. M., McCaughey, J. H., and Bartlett, P. A.: Interannual variability in carbon dioxide exchanges at a boreal wetland in the BOREAS northern study area, *J. Geophys. Res.*, 104, 27663–27672, 1999.
- Krishnan, P., Black, T. A., Barr, A. G., Grant, N. J., Gaumont-Guay, D., and Nesic, Z.: Factors controlling the interannual variability in the carbon balance of a southern boreal black spruce forest, *J. Geophys. Res.*, 113, D09109, doi:10.1029/2007JD008965, 2008.
- Lafleur, P. M., Moore, T. R., Roulet, N. T., and Froelking, S.: Ecosystem respiration in a cool temperate bog depends on peat temperature but not on water table, *Ecosystems*, 8, 619–629, 2005.
- Laiho, R., Vasander, H., Penttilä, T., and Laine, J.: Dynamics of plant-mediated organic matter and nutrient cycling following water-level drawdown in boreal peatlands, *Glob. Biogeochem. Cy.*, 17, 1053, doi:10.1029/2002GB002015, 2003.
- Langergraber, G. and Šimůnek, J.: Modeling variably saturated water flow and multicomponent reactive transport in constructed wetlands, *Vadose Zone J.*, 4, 924–938, 2005.
- Lieffers, V. J.: Sphagnum and cellulose decomposition in drained and natural areas of an Alberta peatland, *Can. J. Soil Sci.*, 68, 755–761, 1988.
- Lieffers, V. J. and Rothwell, R. L.: Effects of drainage on substrate temperature and phenology of some trees and shrubs in an Alberta peatland, *Can. J. For. Res.*, 17, 97–104, 1987.
- Lieffers, V. J. and Macdonald, S. E.: Growth and foliar nutrient status of black spruce and tamarack in relation to depth of water table in some Alberta peatlands, *Can. J. For. Res.*, 20, 805–809, 1990.
- Macdonald, S. E. and Lieffers, V. J.: Photosynthesis, water relations and foliar nitrogen of *Picea mariana* and *Larix laricina* from drained and undrained peatlands, *Can. J. For. Res.*, 20, 995–1000, 1990.
- Minkinen, K., Korhonen, R., Savolainen, I., and Laine, J.: Carbon balance and radiative forcing of Finnish peatlands 1900–2100 – The impact of forestry drainage, *Glob. Change Biol.*, 8, 785–799, 2002.
- Moore, T. R. and Dalva, M.: The influence of temperature and water-table position on carbon dioxide and methane emissions from laboratory columns of peatland soils, *J. Soil Sci.*, 44, 651–664, 1993.
- Moore, T. R. and Roulet, N. T.: Methane flux: Water table relations in Northern wetlands, *Geophys. Res. Lett.*, 20, 587–590, 1993.
- Muhr, J., Höhle, J., Otieno, D. O., and Borcken, W.: Manipulative lowering of the water table during summer does not affect CO₂ emissions and uptake in a fen in Germany, *Ecol. Appl.*, 21, 391–401, 2011.
- Nadelhoffer, K. J., Giblin, A. E., Shaver, G. R., and Laundre, J. A.: Effects of temperature and substrate quality on element mineralization in six arctic soils, *Ecology*, 72, 242–253, 1991.
- Päivänen, J.: Hydraulic conductivity and water retention in peat soils, *Acta Forestalia Fennica*, 129, 1–70, 1973.
- Richardson, A. D., Hollinger, D. Y., Burba, G. G., Davis, K. J., Flanagan, L. B., Katul, G. G., Munger, J. W., Ricciuto, D. M., Stoy, P. C., and Suyker, A. E., Verma, S. B., and Wofsy, S. C.: A multi-site analysis of random error in tower-based measurements of carbon and energy fluxes, *Agric. For. Meteorol.*, 136, 1–18, 2006.
- Saxton, K. E., W. J. Rawls, J. S. Romberger, and Papendick, R. I.: Estimating generalized soil-water characteristics from texture, *Soil Sci. Soc. Am. J.*, 50, 1031–1036, 1986.
- Scanlon, D., and Moore, T. R.: Carbon dioxide production from peatland soil profiles: the influence of temperature, oxic/anoxic conditions and substrate, *Soil Sci.*, 165, 153–160, 2000.
- Shurpali, N. J., Verma, S. B., and Kim, J.: Carbon dioxide exchange in a peatland ecosystem, *J. Geophys. Res.*, 100, 14319–14326, 1995.
- Silvola, J., Alm, J., Ahlholm, U., Nykanen, H., Martikainen, P. J.: CO₂ fluxes from peat in boreal mires under varying temperature and moisture conditions, *J. Ecol.*, 84, 219–228, 1996.
- Sonnentag, O., Chen, J. M., Roulet, N. T., Ju, W., and Govind, A.: Spatially explicit simulation of peatland hydrology and carbon dioxide exchange: Influence of mesoscale topography, *J. Geophys. Res.*, 113, G02005, doi:10.1029/2007JG000605, 2008.
- Sonnentag, O., Kamp, G. V. D., Barr, A. G., and Chen, J. M.: On the relationship between water table depth and water vapor and carbon dioxide fluxes in a minerotrophic fen, *Glob. Change Biol.*, 16, 1762–1776, doi:10.1111/j.1365-2486.2009.02032.x, 2010.
- St-Hilaire, F., Wu, J., Roulet, N. T., Froelking, S., Lafleur, P. M., Humphreys, E. R., and Arora, V.: McGill wetland model: evaluation of a peatland carbon simulator developed for global assessments, *Biogeosciences*, 7, 3517–3530, doi:10.5194/bg-7-3517-2010, 2010.
- Strack, M. and Waddington, J. M.: Response of peatland carbon dioxide and methane fluxes to a water table drawdown experiment, *Global Biogeochem. Cy.*, 21, GB1007, doi:10.1029/2006GB002715, 2007.
- Strack, M., Waddington, J. M., Bourbonniere, R. A., Buckton, E. L., Shaw, K., Whittington, P. and Price, J. S.: Effect of water table drawdown on peatland dissolved organic carbon export and dynamics, *Hydrol. Process.*, 22, 3373–3385, 2008.

- Sulman, B. N., Desai, A. R., Cook, B. D., Saliendra, N., and Mackay, D. S.: Contrasting carbon dioxide fluxes between a drying shrub wetland in Northern Wisconsin, USA, and nearby forests, *Biogeosciences*, 6, 1115–1126, doi:10.5194/bg-6-1115-2009, 2009.
- Sulman, B. N., Desai, A. R., Saliendra, N. Z., Lafleur, P. M., Flanagan, L. B., Sonnentag, O., Mackay, D. S., Barr, A. G., and Kamp, G. V. D.: CO₂ fluxes at northern fens and bogs have opposite responses to inter-annual fluctuations in water table, *Geophys. Res. Lett.*, 37, L19702, doi:10.1029/2010GL044018, 2010.
- Sulman, B. N., Desai, A. R., Schroeder, N. M., Ricciuto, D., Barr, A., Richardson, A. D., Flanagan, L. B., Lafleur, P. M., Tian, H., Chen, G., Grant, R. F., Poulter, B., Verbeeck, H., Ciais, P., Peylin, P., Ringeval, B., Baker, I. T., Schaefer, K., Luo, Y., and Weng, E.: Impact of hydrological variations on modeling of peatland CO₂ fluxes: results from the North American Carbon Program site synthesis, *J. Geophys. Res.–Biogeo.*, in press, 2012.
- Visser, E. J. W., Colmer, T. D., Blom, C. W. P. M., and Voesenek, L. A. C. J.: Changes in growth, porosity, and radial oxygen loss from adventitious roots of selected mono- and dicotyledonous wetland species with contrasting types of aerenchyma, *Plant Cell Environ.*, 23, 1237–1245, 2000.
- Weltzin, J. F., Bridgham, S. D., Pastor, J., Chen, J., and Harth, C.: Potential effects of warming and drying on peatland plant community composition, *Glob. Change Biol.*, 9, 141–151, 2003.
- Wesely, M. L. and Hart, R. L.: Variability of short term eddy-correlation estimates of mass exchange. in: *The forest-atmosphere interaction*, edited by: Hutchinson, B. A., Hicks, B. B., and Reidel, D., Dordrecht, 591–612, 1985.
- Zhang, Y., Li, C., Trettin, C. C., Li, H., and Sun, G.: An integrated model of soil, hydrology, and vegetation for carbon dynamics in wetland ecosystems. *Global Biogeochem. Cy.*, 16, 1061, doi:10.1029/2001GB001838, 2002.